Journal of Applied Mechanics and Technical Physics, Vol. 39, No. 2, 1998

HYPERSONIC FLOW IN AN MHD-ACCELERATION FACILITY AND UNDER FULL-SCALE CONDITIONS

V. I. Alferov and I. V. Egorov

UDC 533.6.011.8

A formulation of the problem, a method of solution, and calculated results are considered for flow past the windward side of a sphere under conditions of an aerodynamic facility (a wind tunnel) with magnetohydrodynamic (MHD) *acceleration of the air flow and the corresponding full-scale flight conditions in the Earth's atmosphere. Calculations were performed on the basis of numerical solution of Navier–Stokes equations taking into account thermochemical nonequilibrium of air and catalytic properties of the body surface. Results of the mathematical simulation of flow around a sphere in an MHD-acceleration wind tunnel are compared with experimental data obtained at the Central Aerohydrodynamic Institute (TsAGI). The problem of recalculation of experimental data for full-scale conditions is analyzed.*

Introduction. One of the main problems of hypersonics is to adequately simulate physical and chemical transformations in the shock layer. Various models of homogeneous and heterogeneous processes that occur in a high-temperature disturbed flow region are considered [1].

Presently, the verification of numerical and experimental data on hypersonic flows in ground-based facilities [2, 3] and under full-scale flight conditions [4] is generating a great deal of interest. Much attention has been given to the search for a more adequate mathematical model for the vibration-dissociation interaction [5, 6] in flow around bodies with arbitrary catalytic activity of the surface [7]. In particular, this includes analysis of the problem of nonequilibrium radiation [4, 8] whose intensity is determined by the concentration of excited particles, the level of excitation of the vibrational degrees of freedom of molecular components, and other factors. The high level of excitation of the electron degrees of freedom of NO molecules immediately behind the shock-wave front leads to intense ultraviolet radiation in the system of gamma-bands (200–230 nm) [9].

For a gas in thermochemical nonequilibrium, the difference in reaction-rate constants suggested by different authors can affect the flow pattern substantially. In this connection, the problem of ground-based verification of both the numerical methods and physicochemical flow models is rather topical. Various types of experimental facilities in which these effects can be reproduced and the methods of investigation of them are reviewed in [10]. Among these facilities, the authors classify shock tubes, expanding shock tubes, and ballistic facilities. The stand-off distance and shape of the shock wave and the pressure distribution over the body are suggested to be used as parameters for comparison between theoretical and experimental results. The short run duration in shock tubes and the small size of models in ballistic ranges impose significant limitations on the experimental study of nonequilibrium processes.

The MHD-gas acceleration hypersonic wind tunnel constructed and used at TsAGI is free of these drawbacks in a sense. It allows one to realize hypersonic flight regimes and to study flow around bodies with a determining influence of physicochemical processes in the shock layer. Alfjorov et al. [11] report some results of comparison of experimental and calculated pressure distributions and results of studying the shock-wave position and shape on the surface of a sphere, a cone, and a wedge for the incoming stream in the MHD

Central Aerohydrodynamic Institute, Zhukovskii 140160. Translated from Prikladnaya Mekhanika i Tekhnicheskaya Fizika, Vol. 39, No. 2, pp. 91–102, March–April, 1998. Original article submitted July 2, 1996.

0021-8944/98/3902-0239 $20.00

facility. It is shown that use of the Navier–Stokes equations yields results that are in better agreement with experiment than those obtained on the basis of the model of a thin viscous shock layer. The shock-wave position and shape and the stand-off distance from the body surface are also described adequately by Navier–Stokes equations with a certain difference between the calculated and experimental values at large distances from the stagnation point. At the same time, the question of whether the MHD-acceleration wind-tunnel conditions correspond to full-scale conditions remained open.

In the present paper, the conditions of flow around bodies in a hypersonic aerodynamic facility with MHD acceleration of the air flow are considered and compared with the corresponding full-scale conditions. Mathematical simulation was based on a solution of the full Navier–Stokes equations. Calculated data are compared with experimental results obtained at TsAGI, and the problem of recalculation of them to experimental data obtained under the full-scale conditions is analyzed.

Governing Equations. In an arbitrary curvilinear coordinate system ξ, η [$x = x(\xi, \eta)$ and $y = y(\xi, \eta)$, where x and y are Cartesian coordinates], the Navier–Stokes equations can be written in divergent form:

$$\frac{\partial \mathbf{Q}}{\partial t} + \frac{\partial \mathbf{E}}{\partial \xi} + \frac{\partial \mathbf{G}}{\partial \eta} = \mathbf{B}.$$

Here $\mathbf{Q}$ is the vector of the conservative dependent variables of the problem, $\mathbf{E}$ and $\mathbf{G}$ are flux vectors in the curvilinear coordinate system, and $\mathbf{B}$ is the source vector. The vectors $\mathbf{Q}$, $\mathbf{E}$, $\mathbf{G}$, and $\mathbf{B}$ are related to the corresponding vectors $\mathbf{Q}_c$, $\mathbf{E}_c$, $\mathbf{G}_c$, and $\mathbf{B}_c$ in the Cartesian coordinate system by the formulas

$$\mathbf{Q} = J\mathbf{Q}_c, \quad \mathbf{E} = J\left(\mathbf{E}_c \frac{\partial \xi}{\partial x} + \mathbf{G}_c \frac{\partial \xi}{\partial y}\right), \quad \mathbf{G} = J\left(\mathbf{E}_c \frac{\partial \eta}{\partial x} + \mathbf{G}_c \frac{\partial \eta}{\partial y}\right), \quad \mathbf{B} = J\mathbf{B}_c,$$

wherein $J = \partial(x, y)/\partial(\xi, \eta)$ is the Jacobian mapping.

The Cartesian coordinates of the vectors $\mathbf{Q}_c$, $\mathbf{E}_c$, $\mathbf{G}_c$, and $\mathbf{B}_c$ for two-dimensional Navier–Stokes equations have the form

$$\mathbf{Q}_c = \begin{Vmatrix} \rho_i \\ \rho u \\ \rho v \\ \rho e \\ \rho_k e_{v,k} \end{Vmatrix}, \quad \mathbf{E}_c = \begin{Vmatrix} \rho_i u + I_x^i \\ \rho u^2 + p + \tau_{xx} \\ \rho uv + \tau_{xy} \\ \rho uH + q_x \\ \rho_k u e_{v,k} + q_{v,x}^k \end{Vmatrix}, \quad \mathbf{G}_c = \begin{Vmatrix} \rho_i v + I_y^i \\ \rho uv + \tau_{xy} \\ \rho v^2 + p + \tau_{yy} \\ \rho vH + q_y \\ \rho_k v e_{v,k} + q_{v,y}^k \end{Vmatrix}, \quad \mathbf{B}_c = \begin{Vmatrix} \omega_i \\ 0 \\ 0 \\ 0 \\ \omega_{v,k} \end{Vmatrix},$$

where ρ_i is the mass density of the ith component of the gas mixture ($i = 1, \ldots, L$, where L is the number of components of the gas mixture). A model of air with $L = 9$ (O_2, N_2, NO, O, N, NO^+, O_2^+, N_2^+, and e^-) is considered in the present paper. In this notation, ρ is the total density of the gas mixture, u and v are the Cartesian coordinates of the velocity vector $\mathbf{V}$, p is the pressure, $e = h - p/\rho + (u^2 + v^2)/2$ is the total energy per unit volume, $H = h + (u^2 + v^2)/2$ is the total enthalpy, $h = \Sigma h_i C_i$ is the static enthalpy of the gas mixture, C_i, ω_i, and h_i are the mass concentrations, rates of formation, and static enthalpies of components of the gas mixture, and $e_{v,k}$ is the specific energy of the vibrational degrees of freedom of diatomic molecules, which is defined in the present paper by the harmonic oscillator formula

$$e_{v,k} = \frac{R}{M_k} \frac{\theta_k}{\exp(\theta_k/T_k) - 1}.$$

Here M_k is the molar weight of the kth component of the gas mixture, R is the universal gas constant, and θ_k and T_k are the characteristic and vibrational temperatures. We used a three-temperature model of vibrational relaxation of the air ($k = 1, \ldots, K$) with $K = 3$, where $k = 1$ corresponds to excitation of the vibrational degrees of freedom of an O_2 molecule, $k = 2$ the same for an N_2 molecule, and $k = 3$ the same for an NO molecule. It was assumed that all the rotational degrees of freedom of the molecules are excited in equilibrium, and the rotational temperatures $T_{r,k}$ coincide with the translational temperature T. The static enthalpies of the atomic components of the gas mixture were determined from the formulas $h_i = (5/2)(R/M_i)T + h_i^0$, and those of the molecular components were determined from the formulas $h_k = (7/2)(R/M_k)T + e_{v,k} + h_k^0$, where h_i^0 is the enthalpy of formation of a component of the gas mixture.

In the flux vectors of the Navier–Stokes equations, τ is the stress tensor with components

$$\tau_{xx} = \mu\left(\frac{2}{3}\,\mathrm{div}\mathbf{V} - 2\,\frac{\partial u}{\partial x}\right), \quad \tau_{xy} = \tau_{yx} = -\mu\left(\frac{\partial u}{\partial y} + \frac{\partial v}{\partial x}\right), \quad \tau_{yy} = \mu\left(\frac{2}{3}\,\mathrm{div}\mathbf{V} - 2\frac{\partial v}{\partial y}\right);$$

q is the heat-flux vector

$$\mathbf{q} = -\lambda\,\mathrm{grad}\,(T) + \tau\mathbf{V} + \sum_{i=1}^{L} h_i^*\mathbf{I}^i + \sum_{k=1}^{K} \mathbf{q}_v^k,$$

where $h_i^* = h_i - e_{v,k}$ is the specific enthalpy of a component of the gas mixture that ignores vibrational energy ($e_{v,k} = 0$ for O and N), $\mathbf{I}^i$ is the diffusion-flux vector of the ith component, determined in the present paper using Fick's law in the approximation of the binary model of diffusion: $\mathbf{I}_i = -\rho D_i\mathrm{grad}\,(C_i)$, $\mathbf{q}_v^k$ is the vibrational energy flux vector of a molecular component, determined from the formula $\mathbf{q}_v^k = -\rho D_v^k\mathrm{grad}\,(C_k e_{v,k})$, and μ, λ, D_i, and D_v^k are the viscosity, thermal conductivity, diffusivity, and self-diffusivity.

In the Navier–Stokes equations for the plane ($\nu = 0$) and axisymmetric ($\nu = 1$) cases, the source vector B has the form

$$\mathbf{B} = J\left(\omega_i, 0, \frac{\nu}{r}\left(p + \mu\left(\frac{2}{3}\,\mathrm{div}\mathbf{V} - 2\,\frac{\nu}{r}\right)\right), 0, \omega_{v,k}\right)^t,$$

where $r = |y|$ is the distance from the symmetry axis.

In the equations for vibrational energy, the source $\omega_{v,k}$ is defined by

$$\omega_{v,k} = Q_{vt,k} + Q_{vv,k} + Q_{vc,k},$$

where $Q_{vt,k}$ are inelastic vibrational–translational interactions, $Q_{vv,k}$ are vibrational–vibrational interactions, and $Q_{vc,k}$ is the effect of chemical reactions on the vibrational relaxation.

In numerical integration of the Navier–Stokes equations, we used the following algebraic relations: the equation of state $p = \rho RT/M$ [$M = (\Sigma C_i/M_i)^{-1}$ is the molar weight of the gas mixture], $\Sigma C_i = 1$, $\Sigma\mathbf{I}^i = 0$, and also the conditions of constant elemental composition and zero diffusion fluxes of elements of the gas mixture, which follow from the binary model of diffusion for a uniform gas mixture. In determining the electron density, it was assumed that the gas is quasi-neutral and ionization is a background process: its contribution was ignored in the total energy balance. This assumption is valid for rates $V_\infty \leqslant$ 8–9 km/sec and is not exactly correct at high rates. Note that the presence of charged particles can significantly affect the transport coefficients.

Boundary Conditions. The problem of supersonic flow past the windward side of a blunted body was solved by distinguishing a bow shock wave in the region bounded by the surface of the body (sphere) $\eta = 0$, the flow centerline $\xi = 0$, the shock-wave surface $\eta = 1$, and the output boundary $\xi = \xi_0$. The coordinates ξ and η were related to the Cartesian coordinates x and y and the variable of the shock wave detachment from the body surface $x^s(\xi)$ by the equations

$$x = x_w(\xi) + x^s(\xi)f(\eta)n_w^x(\xi), \qquad y = y_w(\xi) + x^s(\xi)f(\eta)n_w^y(\xi).$$

Here $x_w(\xi)$ and $y_w(\xi)$ are parametric representations of the surface in flow, $n_w^x(\xi)$ and $n_w^y(\xi)$ are the Cartesian coordinates of the unit vector of the outer normal of the surface, and $f(\eta)$ is a function that defines the condensation of nodes of the computational grid along the normal to the body surface. For a sphere, we have $x_w(\xi) = -\cos(\pi\xi)$ and $y_w(\xi) = \sin(\pi\xi)$.

The generalized Rankine–Hugoniot conditions $\mathbf{G} - \mathbf{G}_\infty = 0$ were specified on the shock wave for $\eta = 1$. The free stream was assumed to consist of molecular nitrogen and oxygen ($C_{O_2} = 0.233$). In calculation of the diffusion component of the flux vector G in the conservation laws on the shock wave, the differential operators were determined from the formulas

$$\frac{\partial}{\partial x} = \frac{\partial\eta}{\partial x}\frac{\partial}{\partial\eta}, \qquad \frac{\partial}{\partial y} = \frac{\partial\eta}{\partial y}\frac{\partial}{\partial\eta}.$$

At the boundary of the computational domain that coincided with the solid body surface $\eta = 0$, we

imposed nonpenetration and slip conditions and the condition of equilibrium-radiation emission

$$q_n + \varepsilon\sigma_r T^4 = 0,$$

where ε is the surface blackness coefficient, σ_r is the Stefan–Boltzmann constant, q_n is the projection of the heat-flux vector $\mathbf{q}$ onto the normal to the body surface. For components of the gas mixture, we used the condition $I_n^i + K_i\rho_i = 0$, where K_i is the coefficient of catalytic activity of the solid-body surface. In all calculations, we used $K_{NO} = 0$ for nitrogen oxide. For vibrational temperatures on the body surface, the equilibrium condition $T_k = T$ was assumed.

For $\xi = 0$, the values of gasdynamic variables on the symmetry axis were determined from the condition of evenness and oddness. At the output boundary of the computational domain we used "mild" conditions of extrapolation of the sought variables $\mathbf{U} = (u, v, p, T, T_k, C_i, x^s)^t$ with an approximation of the form $3\mathbf{U}_k - 4\mathbf{U}_{k-1} + \mathbf{U}_{k-2} = 0$, where $\mathbf{U}$ is the vector of the nonconservative dependent variables of the problem. For the mathematical flow model considered in this paper, $\dim \mathbf{U} = 14$.

The vector of the dependent variables of the problem includes x^s. In solving the problem by an implicit method, we determined x^s using the additional differential equation $\partial x^s/\partial\eta = 0$. To complete the system of boundary conditions on the shock wave, the Rankine–Hugoniot conditions should be supplemented by one more relation [12]. For this we used the condition of extrapolation of pressure from internal points to the shock-wave surface.

Simulation of Chemical Processes. In simulating nonequilibrium chemical processes, we considered the following reactions of dissociation, exchange, and associative ionization:

$$\begin{aligned}
&O_2 + Y \longleftrightarrow 2O + Y, && O + NO \longleftrightarrow N + O_2,\\
&N_2 + Y \longleftrightarrow 2N + Y, && O + N \longleftrightarrow NO^+ + e^-,\\
&NO + Y \longleftrightarrow N + O + Y, && O + O \longleftrightarrow O_2^+ + e^-,\\
&O + N_2 \longleftrightarrow N + NO, && N + N \longleftrightarrow N_2^+ + e^-.
\end{aligned}$$

Here Y is a catalytic particle, which can be a component of the gas mixture. The rate of formation of a component of the gas mixture ω_i was determined from the formula

$$\omega_i = M_i \sum_{l=1}^{20} R_{i,l}$$

using the corresponding reaction rates

$$R_{i,l} = \rho^2(\nu''_{i,l} - \nu'_{i,l})k_{b,l}\Big[K_{c,l}\prod_j X_j^{\nu'_{i,l}} - \prod_j X_j^{\nu''_{i,l}}\Big],$$

where $X_j = C_j/M_j$ is the molar concentration of the jth component, l is the reaction number, and $\nu'_{i,l}$ and $\nu''_{i,l}$ are stoichiometric coefficients. The rates of reverse reactions $k_{b,l}(T)$ and the equilibrium constants $K_{c,l}(T)$ were obtained from the relations in [13].

The effect of nonequilibrium excitation of the vibrational degrees of freedom of the molecules on the dissociation rates was taken into account through the two-temperature dependence of the equilibrium constant $K_{c,l}(T, T_k) = K_{c,l}(T)\Phi_l(T, T_k)$. For the equilibrium constants of the dissociation reactions, the function $\Phi_l(T, T_k)$ was determined on the basis of the model of an effective vibrational level separated by a distance βT (β is the model of dissociation [6]) from the dissociation limit using the formula

$$\Phi_k(T, T_k) = \exp\left(-\frac{D_k}{T}\right)\frac{1 - \exp(-\theta_k/T_k)}{1 - \exp(-\theta_k/T)}\exp\left[-(D_k - \beta_k T)\left(\frac{1}{T_k} - \frac{1}{T}\right)\right].$$

Here D_k is the dissociation energy. The following constants were used in the calculations [6]: D_k = 59,400, 113,200, and 75,500, β_k = 1.5, 3, and 3 for O_2, N_2, and NO, respectively. For the exchange and ionization reactions, the function $\Phi_l(T, T_k)$ was defined as $\Phi_l(T, T_k) = 1$.

Excitation of the Vibrational Degrees of Freedom of the Molecules. The interaction between the vibrational and translational degrees of freedom was simulated using the Landau–Taylor relation

$$Q_{vt,k} = \rho_k[e_{v,k}(T) - e_{v,k}(T_k)]/(\tau_k + \tau_{0,k}),$$

where τ_k is the relaxation time, $\tau_k = 1/(\rho N_A P_k)$, N_A is the Avogadro number, and $P_k = \sum_j p_{k,j}(T)X_j$. The form of the probability functions $p_{k,j}(T)$ was determined from data of [14]. For $T > 8000$ K, we used Park's correction $\tau_{0,k}$ suggested in [15]:

$$\tau_{0,k} = \frac{M}{\rho N_A \sigma \sqrt{8RT/\pi M_k}} \qquad (\sigma = 10^{-20}).$$

The energy exchange between the vibrational degrees of freedom of the molecules was simulated using the expression

$$Q_{vv,k} = \rho^2 N_A C_k \frac{\theta_k R}{M_k} \sum_{\substack{j=1 \\ j\neq k}}^{K} X_j \Theta_{j,k}(T)\left(e^*_{v,j}(1 + e^*_{v,k}) - e^*_{v,k}(1 + e^*_{v,j}) \exp \frac{T_k - T_j}{T}\right).$$

Here $e^*_{v,k} = 1/[\exp(\theta_k/T_k) - 1]$. The form of the functions $\Theta_{j,k}(T)$ was determined from the data of [14].

The change in the vibrational energy of the molecules due to chemical reactions was calculated using the expression

$$Q_{vc,k} = M_k\left(\sum_{l=1}^{15} R_{k,l} \frac{(D_k - \beta_k T)R}{M_k} + \sum_{l=16}^{17} R_{k,l} e_k\right),$$

where the first term is responsible for dissociation reactions [it is assumed that the mean changes in the specific vibrational energy in a single act of dissociation and recombination are $(D_k - \beta_k T)R/M_k$], the second term is responsible for exchange reactions, and the mean change in the specific vibrational energy in a single act of an exchange reaction is assumed to be equal to the specific vibrational energy e_k of a newly formed or vanishing molecule.

Transport Coefficients. To determine the viscosity and thermal conductivity of the gas mixture, we used the following semi-empirical formulas of Wilke [16] and Mason and Saxena [17]:

$$\mu = \sum_i \left(X_i \mu_i \Big/ \left(X_i + \sum_{\substack{j \\ j\neq i}} G_{i,j} X_j\right)\right), \qquad \lambda = \sum_i \left(X_i \lambda_i \Big/ \left(X_i + 1.065 \sum_{\substack{j \\ j\neq i}} G_{i,j} X_j\right)\right).$$

Here $G_{i,j}$ is a function that is given by the equality

$$G_{i,j} = \frac{(1 + \sqrt{\mu_i/\mu_j}\sqrt[4]{M_j/M_i})^2}{2\sqrt{2}\sqrt{1 + M_i/M_j}},$$

and μ_i and λ_i are the viscosity and thermal conductivity of a pure gas:

$$\mu_i = \frac{2.6693 \cdot 10^{-6} T^{0.6472}\sqrt{M_i}}{1.157\sigma_i^2 \varepsilon_i^{0.1472}}, \quad \lambda_i = 3.75 \cdot 10^3 \frac{R\mu_i}{M_i}\left(0.115 + c_{pi} \frac{0.354 \cdot 10^{-3} M_i}{R}\right).$$

The collision diameter σ_i and the parameter ε_i in the potential energy of intermolecular interaction for the neutral components of the gas were found from data of [18]: σ_i = 3.467, 3.798, 3.492, 3.05, and 3.298 and ε_i = 106.7, 71.4, 116.7, 106.7, and 71.4 for O_2, N_2, NO, O, and N, respectively.

The Lennard-Jones potential was used to derive the functional dependence of the transport coefficients [18]. The contribution of the energy due to the rotational degrees of freedom at a temperature T (Eiken's correction) was taken into account in the calculation of the thermal conductivity of the pure gas λ_i.

The diffusion coefficients were determined in the present work from the condition of constant Schmidt numbers $\mathrm{Sm}_i = \mu/(\rho D_i)$ whose values were assumed to be equal to 0.5 for the neutral components of the gas mixture and 0.25 for ions. In determining the self-diffusion coefficients D_v^k in the expression for the vibrational

TABLE 1

Conditions	V_∞, km/sec	ρ_∞, kg/m^3	R_w, m	T_∞, K	$T_{\infty,k}$, K	$C_{O,\infty}$	$C_{N,\infty}$	$C_{NO,\infty}$	$C_{O_2,\infty}$
Tunnel (MHD-facilities)	6.14	$3.23 \cdot 10^{-4}$	0.02	1054	5500	0.231	0.102	0.00068	0.01
Full-scale	7.43	$2.2 \cdot 10^{-4}$	0.0294	240	240	0	0	0	0.233

energy flux, we used the condition of constant numbers $S_k = \mu/(\rho D_v^k)$ whose values were assumed to be equal to 0.5.

Approximation of the Equations. The formulated problem was solved numerically on the basis of an integrointerpolation method (a finite-volume method). Its application to the Navier–Stokes equations written in divergent form permits one to obtain difference analogs of the conservation laws:

$$\frac{\mathbf{Q}_{j,k}^{n+1} - \mathbf{Q}_{j,k}^{n}}{\tau} + \frac{\mathbf{E}_{j+1/2,k}^{n+1} - \mathbf{E}_{j-1/2,k}^{n+1}}{h_\xi} + \frac{\mathbf{G}_{j,k+1/2}^{n+1} - \mathbf{G}_{j,k-1/2}^{n+1}}{h_\eta} = \mathbf{B}_{j,k}^{n+1}.$$

Here n is the time-layer number, j and k are the node numbers in the ξ and η directions, respectively, τ is the time step, and h_ξ and h_η are the steps along the ξ and η coordinates, respectively. This conservative difference scheme is fully implicit and, hence, theoretically allows one to remove the limitations on stability in solution of the rigid system of differential equations.

In approximation of the convective component of the flux vectors $\mathbf{E}$ and $\mathbf{G}$ at semiinteger nodes, we used the second-order central difference scheme $\mathbf{E}_{j+1/2} = (1/2)(\mathbf{E}(\mathbf{Q}_j) + \mathbf{E}(\mathbf{Q}_{j+1}))$. For approximation of the diffusion component of the flux vectors $\mathbf{E}$ and $\mathbf{G}$ on the boundary of an elementary cell, we also used a second-order central difference scheme. The forward and mixed derivatives were calculated using the formulas

$$\frac{\partial \mathbf{U}}{\partial \xi_{j+1/2,k}} = \frac{\mathbf{U}_{j+1,k} - \mathbf{U}_{j,k}}{h_\xi}, \qquad \frac{\partial \mathbf{U}}{\partial \eta_{j+1/2,k}} = \frac{\mathbf{U}_{j+1,k+1} + \mathbf{U}_{j,k+1} - \mathbf{U}_{j+1,k-1} - \mathbf{U}_{j,k-1}}{4h_\eta},$$

where $\mathbf{U}$ is the vector of the nonconservative dependent variables of the problem.

The template of the difference scheme used to approximate the full Navier–Stokes equations consists of nine points. This scheme does not belong to the class of monotonous difference schemes and, hence, cannot be used to solve problems with discontinuities. However, in studies of problems wherein the dependent variables have a smooth behavior, central difference schemes yield more exact results than monotonous schemes (usually the latter do not ensure exact second-order accuracy).

The problem was solved on a nonuniform computational grid. At the upper (shock wave) and lower (solid body surface) boundaries of the computational domain, two zones with thickness $2/\sqrt{\mathrm{Re}}$ were selected. After the grid was made finer, each zone contained 20% of the total number of nodes in the transverse direction.

Solution of Grid Equations. To solve the nonlinear grid equations $\mathbf{F}(\mathbf{X}) = \mathbf{0}$ obtained by approximation of the differential equations, where $\mathbf{X}$ is the vector of the sought grid variables, we used the modified Newton's method

$$\mathbf{X}^{[k+1]} = \mathbf{X}^{[k]} - \tau_{k+1}\mathbf{D}^{-1}\mathbf{F}(\mathbf{X}^k).$$

Here $\mathbf{D} = \partial\mathbf{F}/\partial\mathbf{X}$ is a Jacobi matrix and k is an iteration number. In the course of numerical solution, the parameter τ_k was determined from the formula [19]

$$\tau_{k+1} = \frac{(\Delta\mathbf{X}^{[k]} - \Delta\mathbf{X}^{[k-1]}, \mathbf{X}^{[k]} - \mathbf{X}^{[k-1]})}{(\Delta\mathbf{X}^{[k]} - \Delta\mathbf{X}^{[k-1]})^2},$$

where $\Delta\mathbf{X}^{[k]} = \mathbf{D}^{-1}\mathbf{F}(\mathbf{X}^k)$ is the correction vector. As the iteration process converges, $\tau_k \to 1$ and theoretically the convergence rate tends to the rate of quadratic convergence.

The Jacobi matrix was formed using finite increments of the residual vector with respect to the vector of

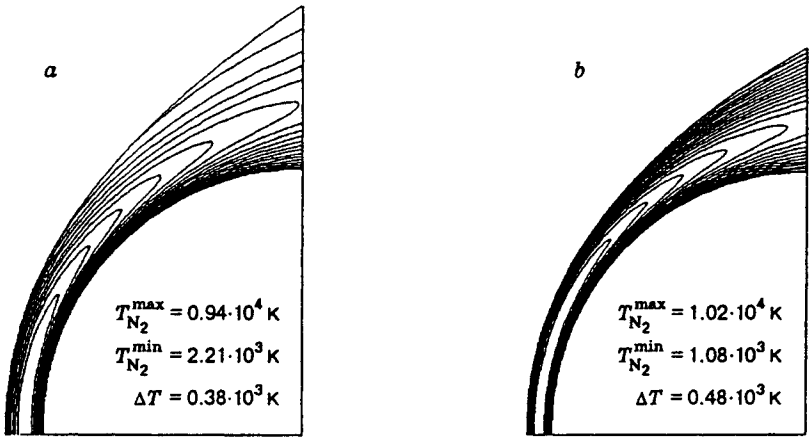

Fig. 1

the sought grid variables. In approximation of the Navier–Stokes equations for a gas mixture in thermochemical nonequilibrium, the operator **D** has a sparse block nine-diagonal structure whose elementary block is a dense 14×14 matrix.

The system of linear algebraic equations obtained by iteration with respect to nonlinearity was solved using the direct method of LU expansion ($\mathbf{D} = \mathbf{L} \times \mathbf{U}$, where **L** is the lower triangular matrix and **U** is the upper triangular matrix). To reduce the total number of arithmetic operations, we analyzed the sparsity pattern of the matrices **L** and **U** and renumbered the unknowns using the method of nested cross sections [20]. This technique has been tested many times in numerical experiments, and its reliability and high efficiency have been confirmed [21, 22].

Calculation Results and Analysis. The numerical studies were performed for the wind-tunnel conditions with MHD acceleration of the air flow and for the corresponding full-scale conditions. The MHD facility operates as follows. The gas heated in an electric-arc heater to $T_0 \sim 3500$ K at $p_0 \sim 2 \cdot 10^5$ Pa enters the mixing chamber, to which an easily ionized eutectic Na additive (~1 wt.%) is introduced. Then through the primary supersonic nozzle the gas enters the MHD accelerator in which it is accelerated to a necessary velocity in crossing d.c. electric and magnetic fields. Expanding in the secondary nozzle to prescribed static parameters, the gas enters the test section in which the model under study is located. After that the gas is discharged into the atmosphere through the diffuser, refrigerator, and a system of ejectors.

Table 1 shows values of the main parameters that characterize the flow for the MHD and full-scale conditions.

The criterion of adequacy of these conditions is the equality of the total enthalpy $H = \text{const}$, the dynamic pressure $q = \text{const}$, and the parameter of binary similarity $D = \text{const}$ ($D = R_w \rho_\infty$, where R_w is the sphere radius). Using these requirements, we found flight conditions in the Earth's atmosphere that correspond to an altitude of $H = 62.7$ km.

The results were obtained for a thermally nonequilibrium air model for two extreme cases of catalytic activity of the body surface: absolutely catalytic and absolutely noncatalytic. The surface blackness coefficient was $\varepsilon = 0.85$. Most of the calculations were performed on a grid containing 31×71 nodes along and normal to the body surface (the coordinates ξ and η). A selective analysis of the accuracy and convergence of data that was performed using a grid with a larger number of nodes showed that the error of determining the equilibrium radiation temperature of the surface was less than 1%.

Figure 1a and b shows isolines of the vibrational temperature of nitrogen T_{N_2} for the experimental and full-scale conditions, respectively (an absolutely catalytic surface). It can be seen that the stand-off distance of the shock wave from the body surface is larger for the MHD conditions than for the flight conditions. This is due to the fact that in the MHD facility the gas flow is partly dissociated and the vibrational degrees of freedom of the molecules are at upper energy levels.

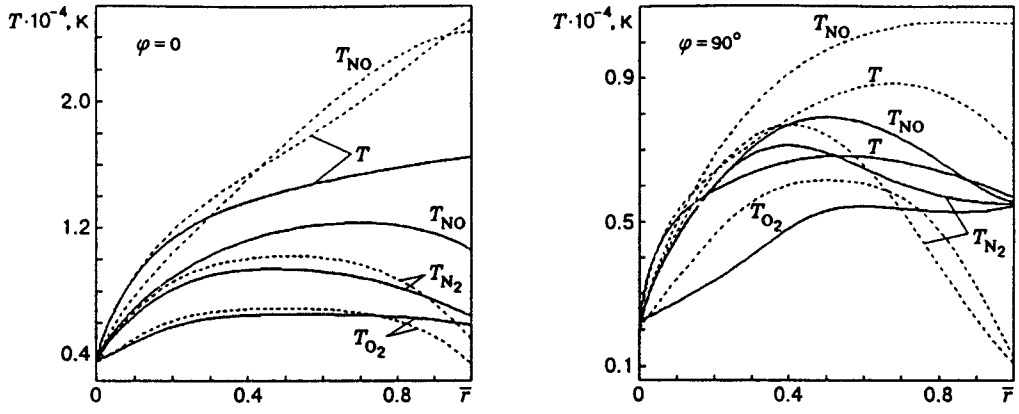

Fig. 2

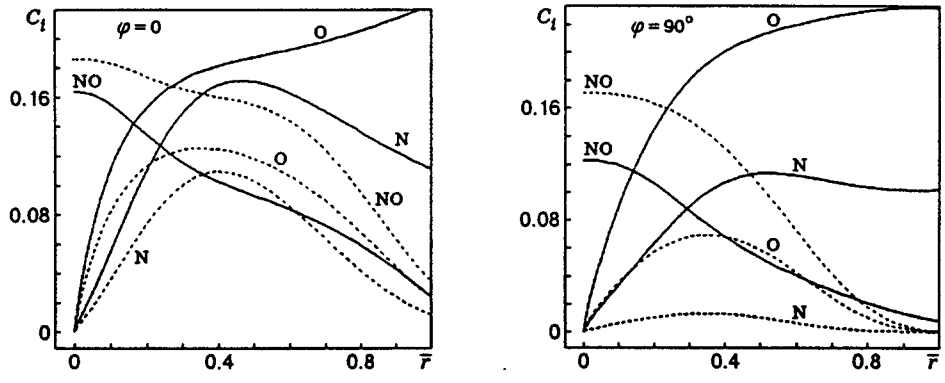

Fig. 3

Profiles of the translational–rotational and vibrational temperatures across the shock layer for two points on the sphere (φ = 0 and 90°) are shown in Fig. 2 (an absolutely catalytic body surface, $\bar{r}$ is the distance from the body surface related to x^s). The solid curves in Figs. 2–6 refer to the MHD conditions and the dashed curves refer to the flight conditions. Evidently, the vibrational temperatures of the O_2 and N_2 molecules are rather close for both conditions, whereas the translational–rotational T and vibrational temperatures of NO differ significantly in the region adjacent to the shock wave and become close in the region of the solid boundary. We can assume that the excitation of the vibrational degrees of freedom of the molecules in the MHD facility is adequate to a certain extent to the excitation under full-scale flight conditions.

To analyze the process of simulation of nonequilibrium chemical processes in the MHD facility, Fig. 3 shows profiles of the mass concentrations of the O, N, and ON components across the shock layer at two points (φ = 0 and 90°). It can be seen that, under flight conditions, the chemical reactions of dissociation proceed more slowly because of the vibration–dissociation interaction.

In laboratory simulations of hypersonic flows, the study of the density of charged particles is very important. Figure 4 shows profiles of the concentrations of charged particles across the shock layer. The body surface was considered absolutely catalytic for the charged particles. According to the data of Fig. 4, there is a great (roughly threefold) difference in electron density near the forward stagnation point, while near the lateral surface, the full-scale and ground-based experimental data are in fairly good agreement.

Figure 5 shows data on the shock-wave detachment from the body surface, obtained by calculations and tests in the facility with MHD acceleration of air. It can be seen from Fig. 5 that the catalytic properties of the body surface affect only slightly the shock wave stand-off distance. The experimental results obtained

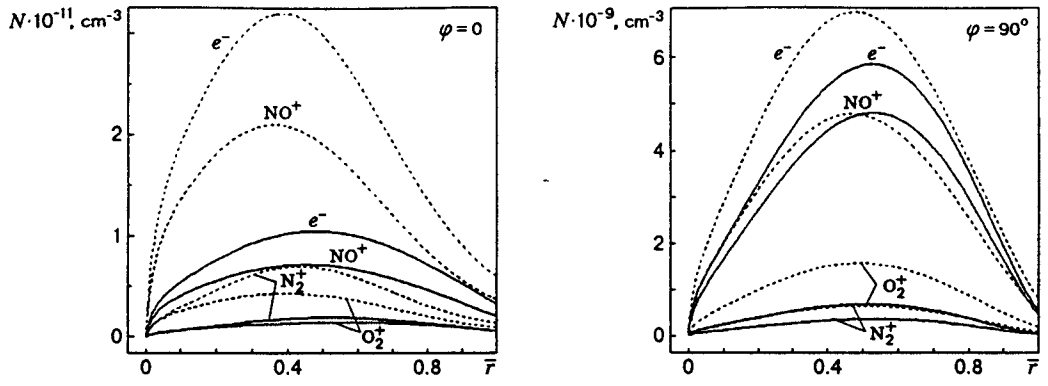

Fig. 4

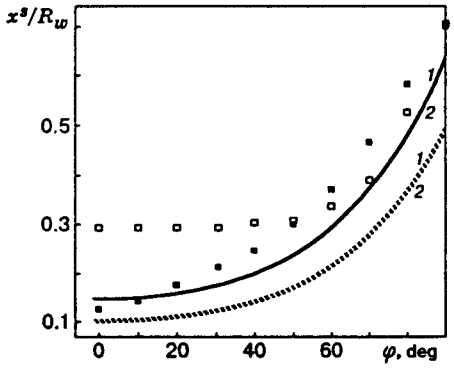

Fig. 5

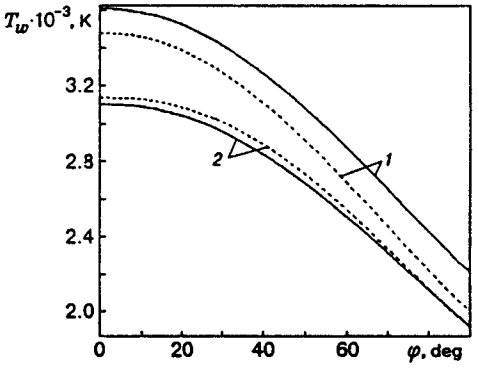

Fig. 6

using the schlieren technique (Fig. 5, closed points) are in good agreement with the calculated data near the stagnation point, and the experimental data are systematically higher than the calculated data downstream of the stagnation point. It is of interest that the luminous zone was highly extended upstream from the shock-wave front near the stagnation point, while in motion downstream from the stagnation point this zone became narrower, reaching values smaller than the data of schlieren pictures. For $\varphi \approx 60$–$80°$, the experimental results for the luminous zone (Fig. 5, open points) are in better agreement with the calculated data for the shock wave stand-off distance. It was noted previously that the shock wave detachment from the body surface is greatly different for the MHD and flight conditions.

Calculated data that characterize the aerodynamic heating of the body surface for the full-scale and MHD conditions are presented in Fig. 6, which shows fair agreement of the heat-transfer data (curves 1 and 2 refer to the catalytic and noncatalytic surface, respectively). The more dramatic effect of the catalytic properties of the body surface for the MHD conditions is explained by the fact that the free-stream gas is partly dissociated and the vibrational degrees of freedom are excited more highly. In this case, the effect of the vibration–dissociation interaction on heat exchange under full-scale conditions is more profound than under the MHD conditions.

This work was supported by the Russian Foundation for Fundamental Research (Grant No. 96-01-00565).

REFERENCES

1. G. A. Tirsky, "Up-to-date gasdynamic models of hypersonic aerodynamic and heat transfer with real gas properties," *Annu. Rev. Fluid Mech.*, **25**, 151–181 (1993).
2. G. Candler, "On the computation of shock shapes in nonequilibrium hypersonic flows," AIAA Paper No. 89-0312, New York (1989).
3. A. Daib, E. Scholl, H. Fruhauf, and O. Knab, "Validation of the URANUS Navier–Stokes code for high-temperature nonequilibrium flows," AIAA Paper No. 93-5070, New York (1993).
4. D. A. Levin, G. V. Candler, R. J. Collins, et al., "Examination of ultraviolet radiation theory for bow shock rocket experiments," AIAA Paper No. 92-2871, New York (1992).
5. Y. Wada, S. Ogawa, and H. Kubota, "Thermo-chemical models for hypersonic flows," *J. Comput. Fluids*, **22**, Nos. 2/3, 179–187 (1993).
6. S. A. Losev, V. N. Makarov, M. Yu. Pogosbekyan, et al., "Thermochemical nonequilibrium kinetic models in strong shock waves on air," AIAA Paper No. 94-1990, New York (1994).
7. S. P. Sharma and C. Park, "A survey of simulation and diagnostic techniques for hypersonic nonequilibrium flows," AIAA Paper No. 87-0406, New York (1987).
8. S. P. Sharma, "Nonequilibrium and equilibrium shock front radiation measurements," AIAA Paper No. 90-0139, New York (1990).
9. V. Gorelov, Gladyshev, A. Kireev, et al., "Nonequilibrium shock-layer radiation in the systems of molecular bands NO and N_2^+ (1−): Experimental study and numerical simulation," AIAA Paper No. 96-1900, New York (1996).
10. V. I. Alfjorov, "A report on the status of MHD hypersonic test technology in Russia," AIAA Paper No. 93-3193, New York (1993).
11. V. I. Alfjorov, I. V. Yegorov, and G. I. Shcherbakov, "On the application of MHD-gas acceleration wind tunnels to investigate hypersonic gas flows over bodies," in: Proc. 33d Symp. on Engineering Aspects of Magnetohydrodynamics, June 13–15, 1995, The University of Tennessee Space Institute, pp. V.2-1–V.2-6.
12. S. R. Chakravarthy, "Euler equations — implicit schemes and boundary conditions," *AIAA J.*, **21**, No. 5, 699–706 (1983).
13. S. W. Kang, W. L. Jones, and M. G. Dunn, "Theoretical and measured electron-density distributions at high altitudes," *AIAA J.*, **11**, No. 2, 141–149 (1973).
14. A. V. Biryukov, "Kinetics of physical processes in gasdynamic lasers," *Tr. Fiz. Inst. Akad. Nauk SSSR*, **83**, 13–86 (1975).
15. C. Park and S. Yoon, "Fully coupled implicit method for thermochemical nonequilibrium air at suborbital flight speeds," *J. Spacecraft*, **28**, No. 1, 31–39 (1991).
16. S. Wilke, "A viscosity equation for gas mixtures," *J. Chem. Phys.*, **18**, No. 4, 517–519 (1950).
17. E. A. Mason and S. C. Saxena, "Approximate formula for the thermal conductivity of gas mixtures," *Phys. Fluids*, **1**, No. 5, 361–369 (1958).
18. J. O. Hirschfeld, C. F. Curtiss, and R. B. Bird, *Molecular Theory of Gases and Liquids*, John Wiley and Sons, New York (1954).
19. T. Kh. Karimov, "On some iterative methods of solving nonlinear equations in the Hilbert space," *Dokl. Akad. Nauk SSSR*, **269**, No. 5, 1038–1042 (1983).
20. A. George, "Nested dissection of a regular finite-element mesh," *SIAM J. Numer. Anal.*, **10**, No. 2, 347–363 (1973).
21. I. V. Egorov, "On the problem of real air properties on integral aerodynamic characteristics," *Izv. Akad. Nauk SSSR, Mekh. Zhidk. Gaza*, No. 4, 156–164 (1992).
22. I. V. Egorov and O. L. Zaitsev, "Development of efficient algorithms for computational fluid dynamic problems," in: *Proc. 5th ISCFD*, Vol. 3, Sendai (1993), pp. 393–400.